Electronic Supplementary Material (ESI) for Journal of Materials Chemistry A.

Supplementary Information

A low-cost "water-in-salt" electrolyte for 2.3 V high-rate carbon-based supercapacitor

Xudong Bu,[1,4,†] Lijun Su,[1,2,†] Qingyun Dou,[1,2,†] Shulai Lei,[1] and Xingbin Yan[1,2,3,*]

[1] Laboratory of Clean Energy Chemistry and Materials, State Key Laboratory of Solid Lubrication, Lanzhou Institute of Chemical Physics, Chinese Academy of Sciences, 730000, P. R. China.
E-mail: xbyan@licp.cas.cn

[2] Center of Materials Science and Opoelectronics Engineering, University of Chinese Academy of Sciences, 100039, P. R. China.

[3] Dalian National Laboratory for Clean Energy, 116023, P. R. China.

[4] School of Material Science and Engineering, Lanzhou University of Technology, 730050, P. R. China.

[†] These authors contributed equally to this work.

[*] Corresponding author: Email: xbyan@licp.cas.cn

Experimental Section

Materials and Characterization

Sodium perchlorate ($NaClO_4$) and potassium acetate (KOAc) were purchased form Sinopharm Chemical Reagent Co. Ltd.. Lithium bis(trifluoromethanesulfonyl) imide (LiTFSI), tetraethylammonium tetrafluoroborate (Et_4NBF_4), acetonitrile (ACN) and propylene carbonate (PC) were purchased from Sigma-Aldrich. Electrolytes were prepared by molality (mol kg^{-1}), which was abbreviated as m. Specifically, $NaClO_4$ salt or LiTFSI salt was mixed with deionized water to prepare aqueous $NaClO_4/H_2O$ (2 m, 5 m, 10 m and 17 m) and LiTFSI/H_2O (21 m) electrolytes. The concentration of two typical commercial organic electrolytes of Et_4NBF_4/ACN and Et_4NBF_4/PC is 1 mol L^{-1} (molarity). In convenience, the molarity of these two commercial electrolytes was converted to molality, which was 1.6 m for Et_4NBF_4/ACN electrolyte and 1.0 m for Et_4NBF_4/PC electrolyte.

The electrochemical stability windows (ESWs) of aqueous $NaClO_4$ electrolytes at different concentrations were measured with cyclic voltammetry (CV) on two stainless steel electrodes between −1.6 V and 1.6 V versus Hg/Hg_2Cl_2 reference electrode at 10 mV s^{-1}. Conductivity of electrolytes was measured by a conductivity meter (DDS-307, YuePing, Shanghai) and viscosity of electrolytes was measured by a glass capillary viscometer. Raman spectroscopy was performed with a High-resolution Raman Spectrometer (HORIBA Jobin Yvon SAS, France).

Electrode Preparation and Electrochemical Measurements

Commercial activated carbon (AC, YP-50F, Kuraray Chemical, Japan) was annealed under argon atmosphere at 700 °C for 3 h prior to use. Electrodes used for the assembly of model supercapacitors (SCs) were prepared by homogeneously mixing 85 wt% AC powder (1.0 mg), 5 wt% carbon black, 5 wt% acetylene black and 5 wt% poly(tetrafluoroethylene) (PTFE, aqueous solution), then the mixture was pressed at 10 MPa on the stainless steel grid current collector and dried at 60 °C for 12 h. Each SC was assembled into a coin cell with two identical AC electrodes with a glass fiber as the separator.

The electrochemical measurements were performed on an electrochemical workstation (CHI660E, Shanghai, China) at room temperature. Each CV or galvanostatic charge/discharge (GCD) test was firstly cycled for ten times to make sure a steady sate of the system before recording data. Electrochemical impedance spectroscopy (EIS) measurement was conducted in a frequency range from 0.01 to 100 kHz with 5 mV amplitude. Cycling performance was tested using a LAND system (CTA2001A, Wuhan Land Electronic Co. Ltd.).

The specific capacitance C (F g^{-1}) of the device was calculated from GCD curve by equation (1):

$$C = \frac{I \cdot \Delta t}{m \cdot \Delta V}, \qquad (1)$$

where I (A) is the loaded current; ΔV (V) = V_o–$V_{IR\text{-}drop}$, V_o (V) is the operation voltage, V_{IR} (V) is the IR drop (or voltage drop) in a GCD test; Δt (s) is the discharge time corresponding to the specified potential change ΔV; m (g) is the total mass loading of

AC in a device.

The energy density E (Wh kg^{-1}) was calculated by equation (2):

$$E = \frac{C \cdot \Delta V^2}{7.2}, \quad (2)$$

The power density P (W kg^{-1}) was calculated using Equation (3):

$$P = \frac{E \cdot 3600}{\Delta t}, \quad (3)$$

In this work, the volume of the electrolyte used in each SC was 0.3 mL, and thus the corresponding price of 0.3 mL electrolyte ($Pr_{0.3mL}$) can be calculated (Table S2). The price-based energy density E_{Pr} (Wh kg^{-1} \$$^{-1}$) was calculated by normalizing the energy density E (Wh kg^{-1}) by the $Pr_{0.3mL}$.

$$E_{Pr} = \frac{E}{Pr_{0.3mL}}, \quad (4)$$

The price-based power density P_{Pr} (W kg^{-1} \$$^{-1}$) was calculated by normalizing the power density P (W kg^{-1}) by the $Pr_{0.3mL}$.

$$P_{Pr} = \frac{P}{Pr_{0.3mL}} \quad (5)$$

Density-functional-theory-based molecular dynamics (DFT-MD) simulations

DFT-MD simulations were performed in the NVT ensemble at 300 K with a time step of 1.0 fs. All the simulations were carried out by using the projector augmented wave (PAW) pseudopotentials as implemented in the Vienna *ab initio* simulation package (VASP).[1,2] The Perdew–Burke–Ernzerhof (PBE) parametrization of the generalized gradient approximation (GGA) was adopted for the exchange correlation potential.[3] A cubic box with $1 \times 1 \times 0.9$ nm^3 filled with one Na^+, one ClO_4^- and 28

H_2O was built in order to simulate 2 m $NaClO_4$ electrolyte, while a cubic box with $1.1\times1.1\times1.2$ nm^3 filled with 8 Na^+, 8 ClO_4^- and 24 H_2O was adopted in order to simulate 17 m $NaClO_4$ electrolyte.

Table S1. The prices of salts and solvents we used in this study, which were obtained from different chemical reagent companies.

Salts/ Solvents	CAS No.	Companies								
		Sigma Aldrich			Alfa Aesar			TCI		
		Stock No.	Pack Size	Price ($)	Stock No.	Pack Size	Price ($)	Stock No.	Pack Size	Price ($)
$NaClO_4$	7601-89-0	410241	100g	49.00	11623-22	100g	35.00	--	--	--
		410241	500g	160.00	11623-36	500g	96.90	--	--	--
LiTFSI	90076-65-6	544094	5g	35.90	H27307-09	10g	61.30	B2542	25g	75.00
		544094	25g	112.00	H27307-18	50g	184.00	B2542	250g	440.00
Et_4NBF_4	429-06-1	86618	5g	73.50	A10211-06	5g	26.50	T0983	5g	26.00
		86618	25g	257.00	A10211-18	50g	103.00	T0983	25g	79.00
ACN	75-05-8	271004	100mL	62.50	42311-AK	250mL	27.60	A0060	25mL	15.00
		271004	1L	119.00	42311-K2	1L	70.30	A0293	100mL	45.00
PC	108-32-7	310328	100mL	53.50	A15552-30	250g	20.80	P0525	25g	14.00
		310328	500mL	65.50	A15552-0B	1000g	41.10	P0525	500g	30.00

Table S2. The prices of different electrolytes, which were calculated based on the price data from Sigma Aldrich.

Electrolytes	17 m $NaClO_4/H_2O$	21 m $LiTFSI/H_2O$	1.6 m Et_4NBF_4/ACN	1.0 m Et_4NBF_4/PC
Price ($ g^{-1})	0.33	6.16	4.20	3.03
Price ($ mL^{-1})	0.55	11.15	3.61	3.64
$Pr_{0.3mL}$ ($)	0.17	3.35	1.08	1.09

In our study, the prices of the smallest pack size of salts and solvents form Sigma Aldrich were chosen to calculate the cost of the electrolytes. Aqueous electrolytes ignored the cost of the water, while non-aqueous electrolytes included the cost of the organic solvents. $Pr_{0.3mL}$ denoted the price of electrolyte of 0.3 mL, which was the volume used in each coin SC.

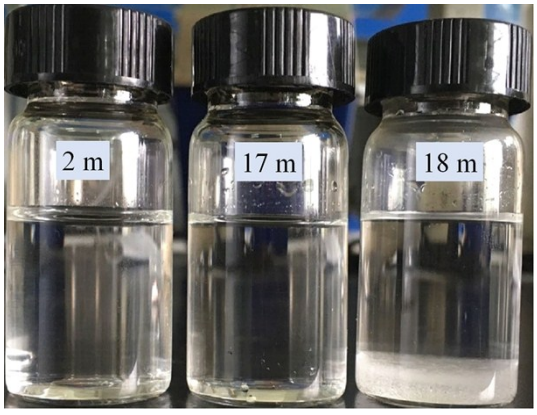

Figure S1. Photographs of $NaClO_4$ aqueous solutions with different concentrations. It should be mentioned that 18 m $NaClO_4$ solution could not be obtained because $NaClO_4$ salt was not fully dissolved in it.

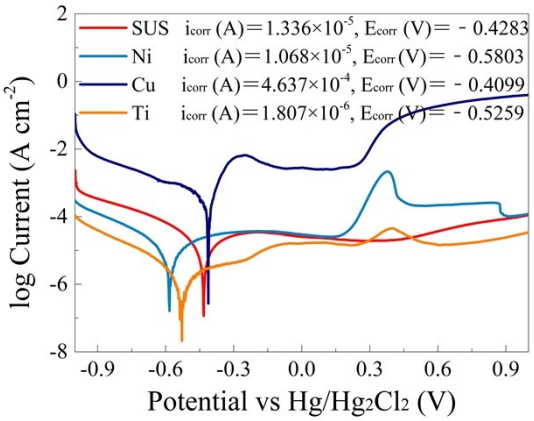

Figure S2. Tafel curves of four different electrodes of stainless steel (SUS), nickel (Ni), copper (Cu) and titanium (Ti) in 17 m $NaClO_4$ solution at ambient temperature.

The electrochemically corrosive feature of different electrodes in 17 m $NaClO_4$ solution was tested by Tafel curves, and the estimated corrosion current densities (i_{corr}) and corrosion potentials (E_{corr}) for all tested electrodes are listed in Figure S2. The intersection point of the vertical line through corrosion potential and the extrapolated linear portions of the anodic and cathodic polarizations in Tafel curves were used to estimate the value of the corrosion current density.[4,5] The copper and nickel electrodes showed a significant increase in current density due to pitting corrosion at ~0.3 V, indicating a relatively poor electrochemical stability in the solution. Compared with stainless steel, although the corrosion current density of titanium was smaller, its corrosion potential was more negative. Thus, stainless steel could be served as the best current collector in aqueous $NaClO_4$ electrolyte.

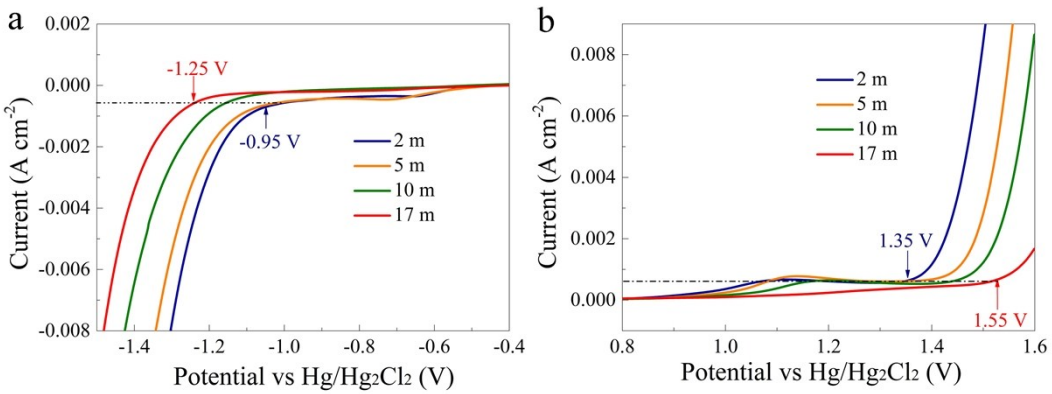

Figure S3. ESWs of aqueous $NaClO_4$ electrolytes zoomed in (a) cathodic and (b) anodic regions.

In this system, we defined a value of 0.6 mA cm^{-2} as the threshold of electrolyte decomposition.

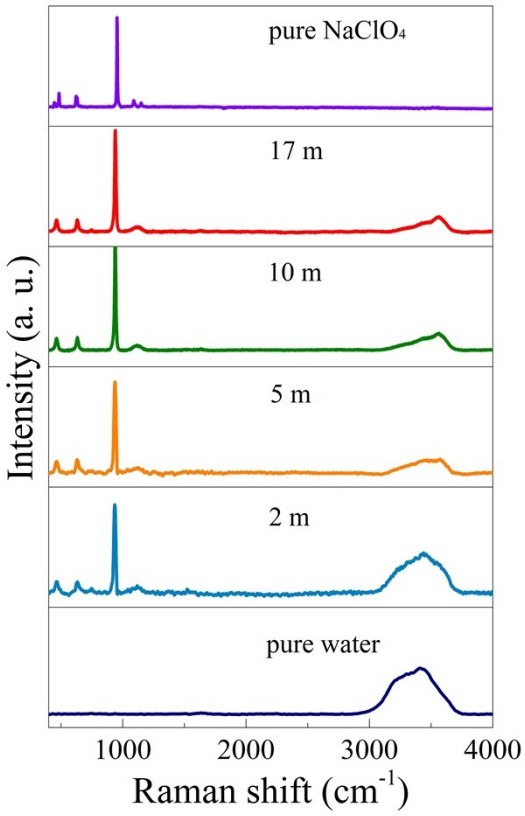

Figure S4. Raman spectra of aqueous $NaClO_4$ electrolytes at different concentrations with pure $NaClO_4$ salt and pure water as the references.

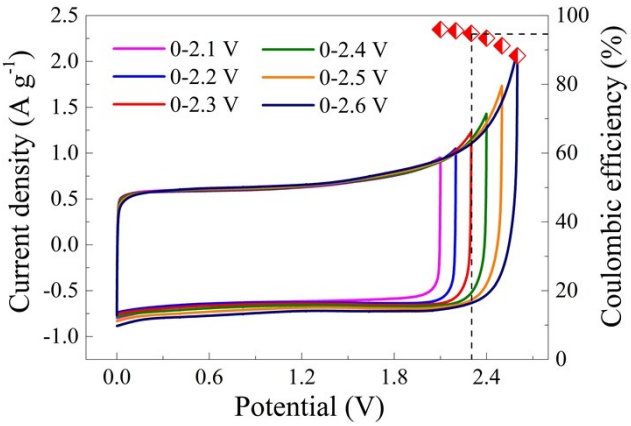

Figure S5. CV curves of the SC using YP-50F electrodes and 17 m $NaClO_4$ electrolyte at a scan rate 20 mV s^{-1} at different operation voltages of 2.1, 2.2, 2.3, 2.4, 2.5 and 2.6 V.

By analyzing the CV curves, the suitable maximum operation voltage of SC using YP-50F electrodes and 17 m $NaClO_4$ electrolyte was 2.3 V, beyond which the coulombic efficiency of CV curves was below 95%.

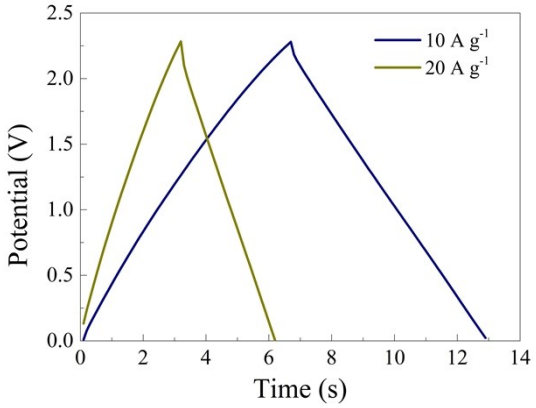

Figure S6. The GCD curves of the model SC using 17 m $NaClO_4$ electrolyte at large current densities of 10 and 20 A g^{-1}, respectively.

The IR drops in the GCD curves were resulted from the internal resistance of SC, which generally increased with the elevated current densities.[6] The IR drops of the SC using 17 m $NaClO_4$ electrolyte were evidently smaller than those using 21 m LiTFSI/H_2O electrolyte, 1.6 m Et_4NBF_4/ACN electrolyte and 1.0 m Et_4NBF_4/PC electrolyte, as shown in Figure S8-S10.

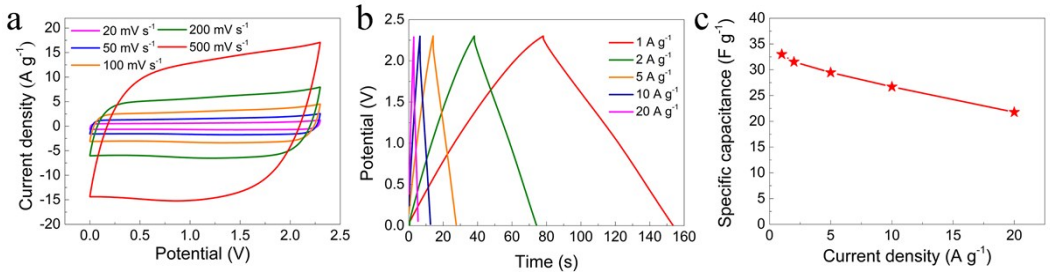

Figure S7. Electrochemical performance of 2.3 V SC using YP-50F electrodes and 17 m $NaClO_4$ electrolyte with a five-fold increase of active materials per unit area. (a) CV curves at different scan rates. (b) GCD curves at different current densities. (c) Rate capability.

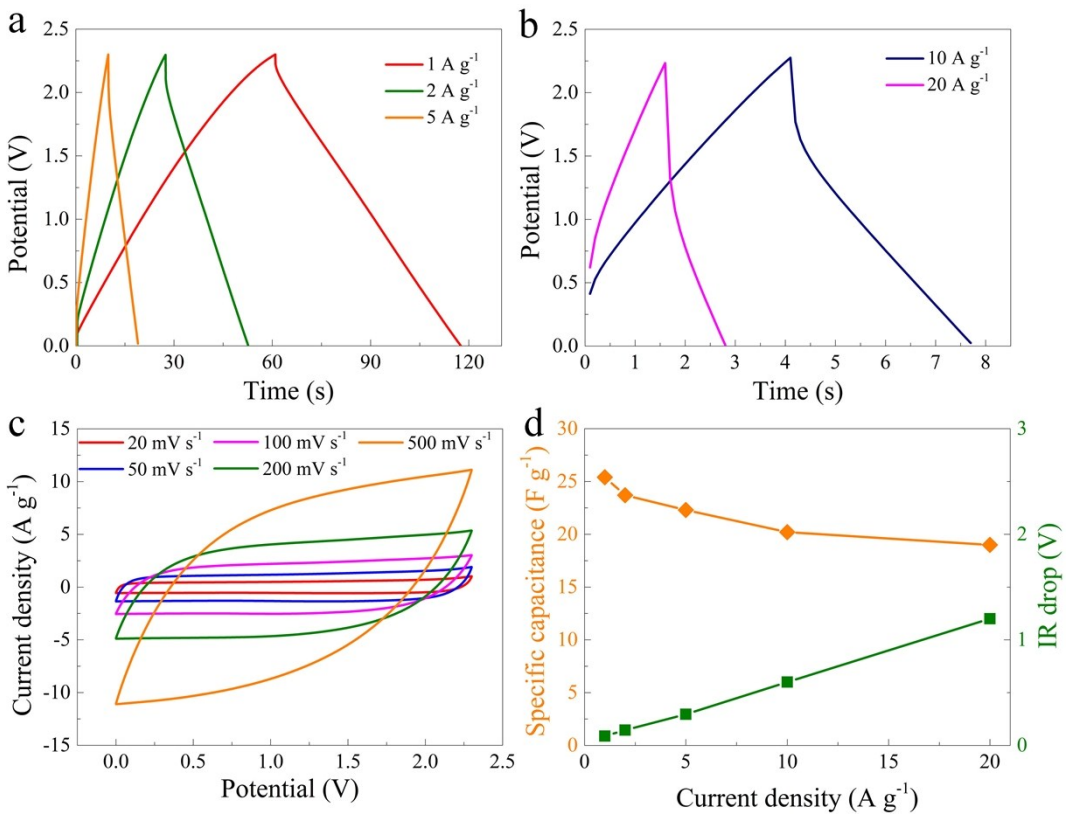

Figure S8. Electrochemical performance of the SC using 21 m LiTFSI/H_2O electrolyte at an operation voltage of 2.3 V. (a) and (b) GCD curves at different current densities. (c) CV curves at different scan rates. (d) Specific capacitance and IR drop at different current densities.

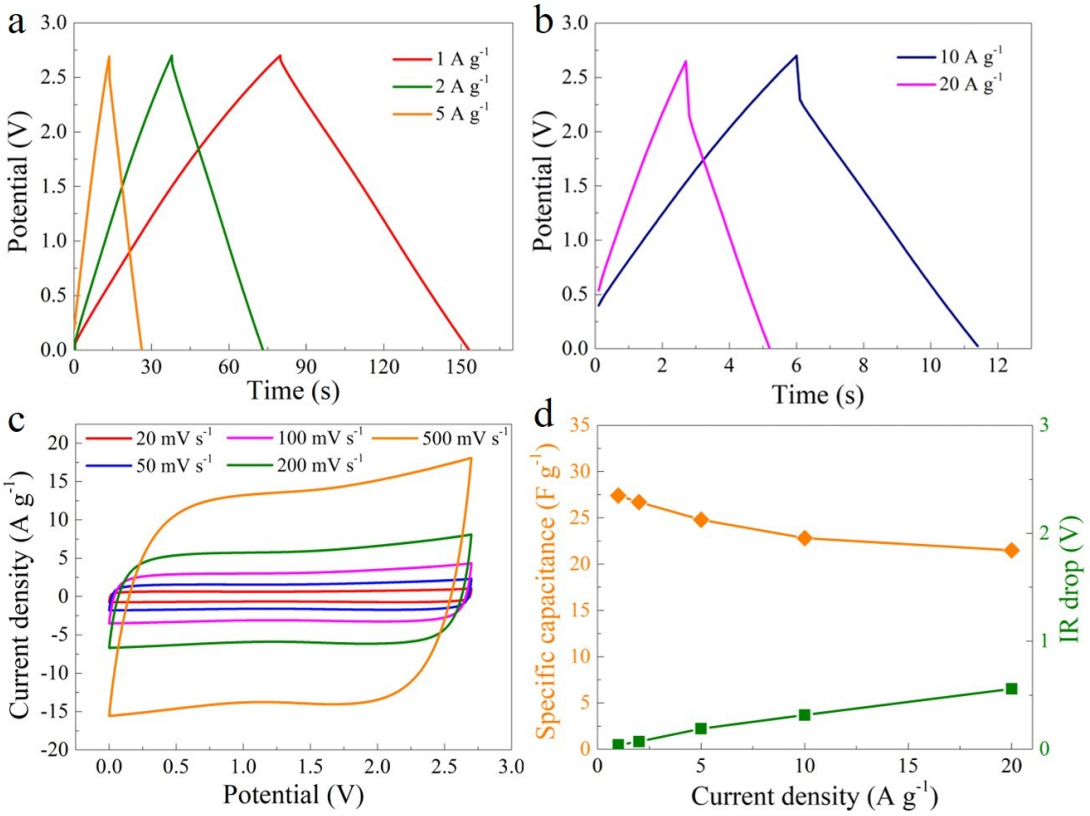

Figure S9. Electrochemical performance of the SC using nonaqueous 1.6 m Et_4NBF_4/ACN electrolyte at an operation voltage of 2.7 V. (a) and (b) GCD curves at different current densities. (c) CV curves at different scan rates. (d) Specific capacitance and IR drop at different current densities.

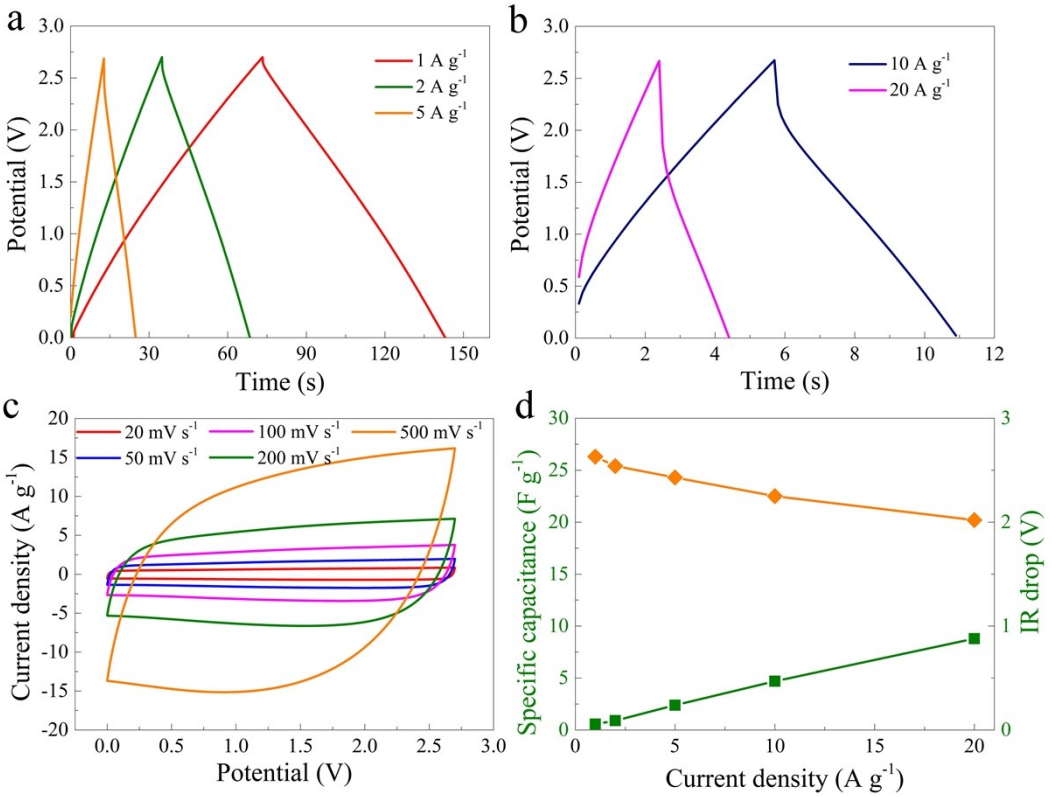

Figure S10. Electrochemical performance of the SC using nonaqueous 1.0 m Et_4NBF_4/PC electrolyte at an operation voltage of 2.7 V. (a) and (b) GCD curves at different current densities. (c) CV curves at different scan rates. (d) Specific capacitance and IR drop at different current densities.

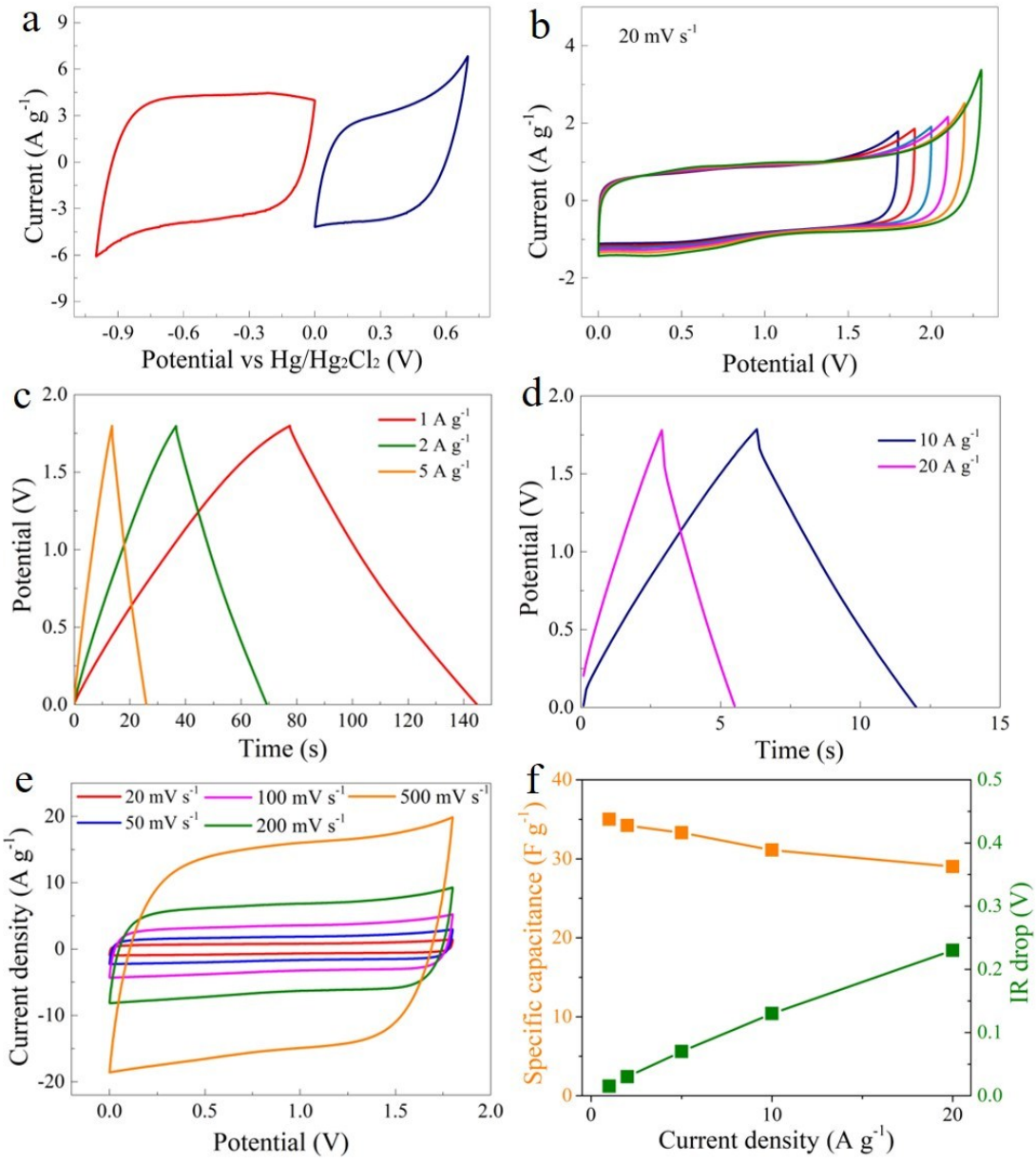

Figure S11. (a) CV curves of YP-50F electrode in 27 m KOAc electrolyte, which were obtained by scanning from the open circuit potential to positive and to negative polarization ranges at a scan rate of 20 mV s^{-1}, respectively. (b) CV curves of the SC using 27 m KOAc WIS electrolyte at a scan rate of 20 mV s^{-1} at different operation voltages. By analyzing the CV curves shown in (b), the suitable maximum operation voltage of SC was 1.8 V. Electrochemical performance of the SC using nonaqueous 27 m KOAc electrolyte at an operation voltage of 1.8 V. (c) and (d) GCD curves at different current densities. (e) CV curves at different scan rates. (f) Specific capacitance

and IR drop at different current densities.

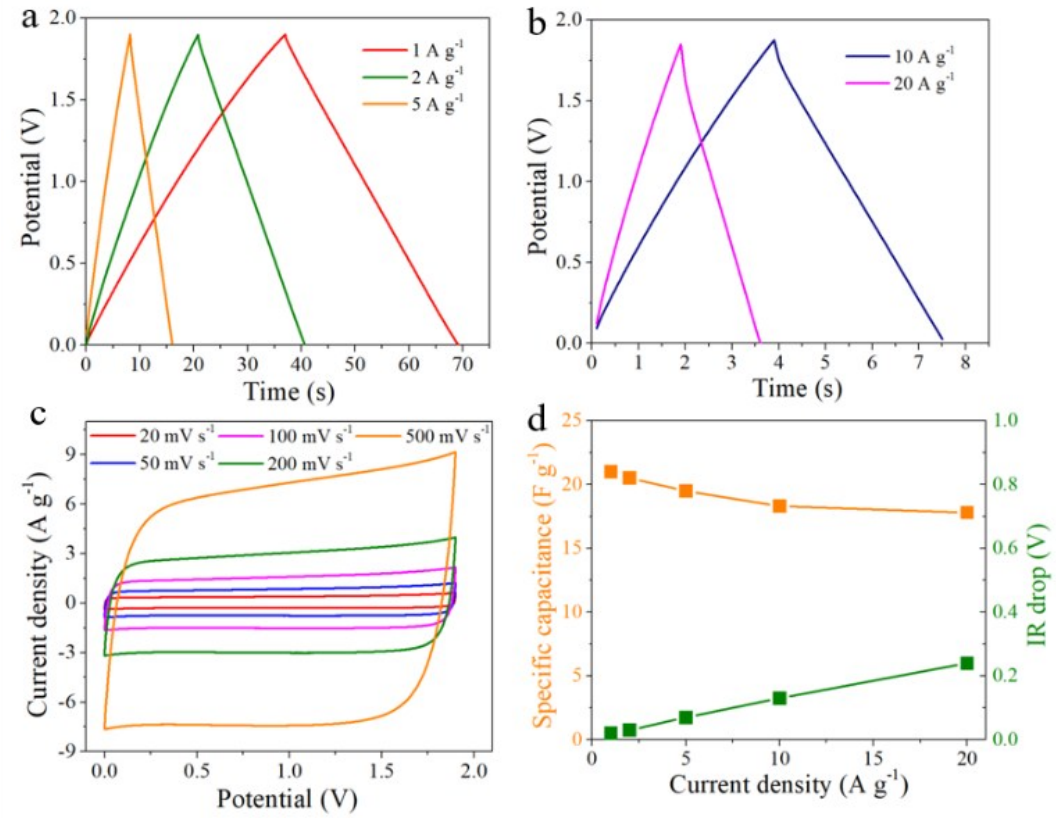

Figure S12. Electrochemical performance of the SC using 1.0 m Li_2SO_4 electrolyte at an operation voltage of 1.9 V. (a) and (b) GCD curves at different current densities. (c) CV curves at different scan rates. (d) Specific capacitance and IR drop at different current densities.

References

1. G. Kresse and J. Furthmüller, *Phys. Rev. B: Condens. Matter Mater. Phys.*, 1996, **54**, 11169-11186.
2. G. Kresse and J. Furthmu¨ller, *Comput. Mater. Sci.*, 1996, **6**, 15-50.
3. J. P. Perdew, K. Burke and M. Ernzerhof, *Phys. Rev. Lett.*, 1996, **77**, 3865-3868.
4. Y. Liu, S. Li, J. Zhang, J. Liu, Z. Han and L. Ren, *Corros. Sci.*, 2015, **94**, 190-196.
5. P. Mourya, P. Singh, A. K. Tewari, R. B. Rastogi and M. M. Singh, *Corros. Sci.*, 2015, **95**, 71-87.
6. S. Zhang and N. Pan, *Adv. Energy Mater.* 2014, **4**, 1401401.